Author(s): Rissanen, Antti-Pekka E.; Mikkola, Tom; Gagnon, Dominique D.; Lehtonen, Elias; Lukkarinen, Sakari; Peltonen, Juha E.

Title: Wagner diagram for modeling O2 pathway : calculation and graphical display by the Helsinki O2 Pathway Tool

Year: 2024

Version: Published version

Please cite the original version:

Rissanen, A.-P. E., Mikkola, T., Gagnon, D. D., Lehtonen, E., Lukkarinen, S., & Peltonen, J. E. (2024). Wagner diagram for modeling O2 pathway : calculation and graphical display by the Helsinki O2 Pathway Tool. Physiological Measurement, 45(5), Article 055028. https://doi.org/10.1088/1361-6579/ad4c36

Physiological Measurement

IPEM
Institute of Physics and Engineering in Medicine

PAPER • OPEN ACCESS

Wagner diagram for modeling O_2 pathway—calculation and graphical display by the Helsinki O_2 Pathway Tool

To cite this article: Antti-Pekka E Rissanen *et al* 2024 *Physiol. Meas.* **45** 055028

IOP Publishing Physiol. Meas. 45 (2024) 055028 https://doi.org/10.1088/1361-6579/ad4c36

Physiological Measurement

IPEM Institute of Physics and Engineering in Medicine

OPEN ACCESS

RECEIVED
26 November 2023

REVISED
3 May 2024

ACCEPTED FOR PUBLICATION
15 May 2024

PUBLISHED
4 June 2024

PAPER

Wagner diagram for modeling O_2 pathway—calculation and graphical display by the Helsinki O_2 Pathway Tool

Antti-Pekka E Rissanen[1,2,6,*], **Tom Mikkola**[1,3,6], **Dominique D Gagnon**[1,2,4,5], **Elias Lehtonen**[1,2], **Sakari Lukkarinen**[3] **and Juha E Peltonen**[1,2]

[1] Helsinki Sports and Exercise Medicine Clinic, Foundation for Sports and Exercise Medicine (HULA), Helsinki, Finland
[2] Sports and Exercise Medicine, Faculty of Medicine, University of Helsinki, Helsinki, Finland
[3] School of Information and Communication Technology, Metropolia University of Applied Sciences, Helsinki, Finland
[4] Faculty of Sports and Health Sciences, University of Jyväskylä, Jyväskylä, Finland
[5] School of Kinesiology and Health Sciences, Laurentian University, Sudbury, ON, Canada
[6] Contributed equally to the study.
[*] Author to whom any correspondence should be addressed.

E-mail: antti-pekka.rissanen@helsinki.fi

Keywords: convection, diffusion, exercise, Fick, HO_2PT, oxygen

Supplementary material for this article is available online

Abstract

Objective. Maximal O_2 uptake ($\dot{V}O_{2max}$) reflects the individual's maximal rate of O_2 transport and utilization through the integrated whole-body pathway composed of the lungs, heart, blood, circulation, and metabolically active tissues. As such, $\dot{V}O_{2max}$ is strongly associated with physical capacity as well as overall health and thus acts as one predictor of physical performance and as a vital sign in determination of status and progress of numerous clinical conditions. Quantifying the contribution of single parts of the multistep O_2 pathway to $\dot{V}O_{2max}$ provides mechanistic insights into exercise (in)tolerance and into therapy-, training-, or disuse-induced adaptations at individual or group levels. We developed a desktop application (Helsinki O_2 Pathway Tool—HO_2PT) to model numerical and graphical display of the O_2 pathway based on the 'Wagner diagram' originally formulated by Peter D. Wagner and his colleagues. *Approach.* The HO_2PT was developed and programmed in Python to integrate the Fick principle and Fick's law of diffusion into a computational system to import, calculate, graphically display, and export variables of the Wagner diagram. *Main results.* The HO_2PT models O_2 pathway both numerically and graphically according to the Wagner diagram and pertains to conditions under which the mitochondrial oxidative capacity of metabolically active tissues exceeds the capacity of the O_2 transport system to deliver O_2 to the mitochondria. The tool is based on the Python open source code and libraries and freely and publicly available online for Windows, macOS, and Linux operating systems. *Significance.* The HO_2PT offers a novel functional and demonstrative platform for those interested in examining $\dot{V}O_{2max}$ and its determinants by using the Wagner diagram. It will improve access to and usability of Wagner's and his colleagues' integrated physiological model and thereby benefit users across the wide spectrum of contexts such as scientific research, education, exercise testing, sports coaching, and clinical medicine.

1. Introduction

Maximal O_2 uptake ($\dot{V}O_{2max}$) is one of the most ubiquitous measures in human health and a fundamental pillar upon which the field of exercise science and medicine has evolved over the last century. The concept, according to which an individual possesses a finite rate of O_2 transport and utilization within an integrated pathway extending from the environment to the mitochondria to support the individual's maximal rate of whole-body oxidative metabolism, has a central role in evolutionary history (Koch and Britton 2008). Contemporarily, well-acknowledged associations of oxidative metabolism with both physical capacity and

overall health enable the extensive use of $\dot{V}O_{2max}$ as one predictor of physical performance and risks for morbidity and mortality in populations ranging from elite athletes to clinical patients (Levine 2008, Ross *et al* 2016, Millet *et al* 2023).

Oxygen transport from the atmosphere to the mitochondria follows a well-established sequence: (i) ventilation of inspired air from the atmosphere to the pulmonary alveoli, (ii) diffusion of O_2 from alveolar gas into the pulmonary capillary blood, (iii) convective O_2 transport from the pulmonary capillary bed to the pulmonary veins, left heart, and further to the microvasculature of target tissues, and finally, (iv) unloading of O_2 from erythrocytes' hemoglobin (Hb) in microvasculature and subsequent passive O_2 diffusion to the mitochondria, where O_2 is used to produce ATP via oxidative phosphorylation (Wagner 2008, 2011, 2020, 2023). The Fick principle equation (equation (1)) expresses parametric limits and physiological characteristics of $\dot{V}O_{2max}$ and is historically one of the first attempts to define the O_2 transport cascade (Fick 1870):

$$\dot{V}O_2 = \dot{Q} \times C(a\text{-}v)O_2 \tag{1}$$

where $\dot{V}O_2 = O_2$ uptake, $\dot{Q}$ = cardiac output, and $C(a\text{-}v)O_2$ = arterial-venous O_2 difference.

Unfortunately, the Fick principle equation fails to distinguish detailed limitations/improvements/declines in the O_2 cascade sequence from inspired air to the mitochondria. While the effect of $\dot{Q}$ on $\dot{V}O_2$ is simplistic in nature, challenges arise when interpreting $C(a\text{-}v)O_2$ (Gifford *et al* 2024). This is because $C(a\text{-}v)O_2$ is affected by numerous factors such as pulmonary ventilation, matching of ventilation to $\dot{Q}$, diffusion of O_2 from the alveoli into the pulmonary circulation, affinity of Hb for O_2, total Hb mass and blood volume (determining Hb concentration [Hb]), $\dot{Q}$, systemic and local control of blood flow, number and size of capillaries, hematocrit in capillaries, diffusion of O_2 from the microvasculature into metabolically active cells and their mitochondria, mitochondrial density, and oxidative enzyme activity (Rowell 1986, Poole *et al* 2022).

To overcome the obstacles of using the Fick principle equation alone, Peter D. Wagner and his colleagues presented an integrated model roughly 30 years ago to characterize how all transport steps contribute to $\dot{V}O_{2max}$ (Roca *et al* 1989, Wagner 1991, 1992). Their key contribution to existing knowledge was in merging Fick's law of diffusion, presented in equation (2) and expressing peripheral O_2 diffusion from capillaries to mitochondria, with the Fick equation to integrate different components of the O_2 pathway with each other,

$$\dot{V}O_2 = DO_2 \times (PcapO_2 - PmitoO_2) \tag{2}$$

where DO_2 = diffusive O_2 conductance, $PcapO_2$ = partial capillary O_2 pressure, and $PmitoO_2$ = partial mitochondrial O_2 pressure.

Equation (2) can be simplified by two assumptions. First, as $PmitoO_2$ is around 1–3 mmHg during (near) maximal exercise, and partial microvascular O_2 pressure is estimated to be between those of arteries (~90–100 mmHg) and veins (~20–40 mmHg), making the mean $PcapO_2$ to be commonly about 35–50 mmHg, $PmitoO_2$ is substantially lower than $PcapO_2$ and can thus be assumed to be algebraically zero (Gayeski and Honig 1986, Roca *et al* 1989, Richardson *et al* 1995). Second, $PcapO_2$ may be replaced with a constant, k, multiplied by partial venous O_2 pressure (PvO_2). This is because PvO_2 is proportional to $PcapO_2$, when DO_2 is assumed to be uniform along the capillaries with homogeneous blood flow distribution (Roca *et al* 1989). Consequently, Fick's law of diffusion can be presented as follows (equation (3)) (Wagner 2011):

$$\dot{V}O_2 = DO_2 \times k \times PvO_2. \tag{3}$$

As originally presented by Wagner and his colleagues, the Fick principle and the presented form of Fick's law of diffusion (i.e. equations (1) and (3), respectively) can be graphically displayed as a relationship between $\dot{V}O_2$ and PvO_2 (figure 1). While the described system and equations (1) and (2) apply equally from rest to maximal exercise, it is only from near-maximal to maximal exercise that the graphical display is appropriate for the necessary assumptions to apply. This particularly means that $PmitoO_2$ must be low enough to have a negligible influence on the calculations (Gayeski and Honig 1986, Richardson *et al* 1995), which enables the use of equation (3). In other words, the approach presented here and the graphical display pertain only to conditions under which the oxidative capacity of the metabolically active tissues' mitochondria exceeds the capacity of the O_2 transport system to deliver O_2 to the mitochondria.

Wagner's and his colleagues' conflation of the Fick principle and Fick's law of diffusion to the '*Wagner diagram*' exemplifies whole-body cooperativity between perfusive (Fick principle) and diffusive (Fick's law) processes from pulmonary ventilation to skeletal muscles (Wagner 2008, 2011, 2020, 2023, Esposito *et al* 2010). To understand O_2 transport, every step of the pathway must be considered simultaneously instead of approaching them separately, and no single step can solely be the factor limiting $\dot{V}O_{2max}$. Mathematically,

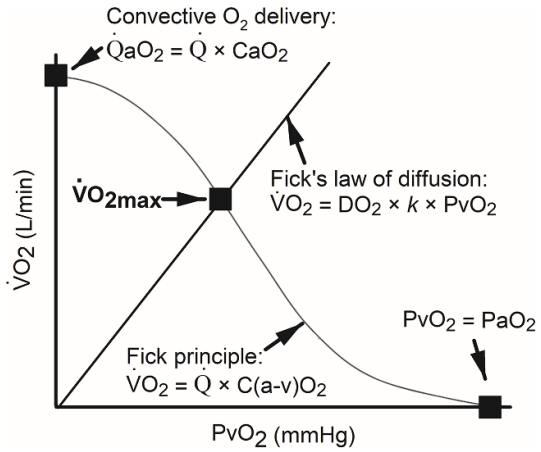

Figure 1. Schematic graphical display of the relationship between O_2 uptake ($\dot{V}O_2$) and partial venous O_2 pressure (PvO_2). The Fick principle, represented by the curved line, and Fick's law of diffusion, represented by the straight line, are conflated to yield a given maximal $\dot{V}O_2$ ($\dot{V}O_{2max}$) for the given conditions at the intersection of the two lines. See text for details and table 1 for the abbreviations.

conservation of O_2 mass is maintained at every step, and the two conservation of mass equations (i.e. Fick principle and Fick's law of diffusion) can be solved simultaneously to provide a quantitative understanding of how the transport processes function together, how each step affects overall transport, and in particular, how O_2 transport and utilization eventually reach their limits so that the conservation of O_2 mass equations eventually result in the same $\dot{V}O_2$ at the same PvO_2 (Wagner 2020, 2023). This model can be and has been utilized in health and disease and its underlying physiology has been extensively clarified (Poole and Richardson 1997, Poole and Musch 2008, Hirai *et al* 2015, Poole *et al* 2021, 2022).

Although $\dot{V}O_2$ measurements along with development and validation of invasive and noninvasive $\dot{Q}$ measurements have provided an access to the Wagner diagram for decades, an easy access to quantify all key variables of the O_2 pathway has been a challenge. Recently, however, both Houstis *et al* (2018) and Legendre *et al* (2021) have provided detailed steps for O_2 pathway calculation. Similarly, a web-based calculator (https://bakersportscardiology.shinyapps.io/fitoxy/) presented by Howden *et al* (2021) allows independent calculation of O_2 pathway steps. Furthermore, Pilotto *et al* (2022) and Manferdelli *et al* (2023) have very recently presented near-infrared spectroscopy-based methods providing functional estimates of muscle DO_2 in exercising humans. However, to our knowledge, these advances have yet to be integrated into a comprehensive system, or tool, providing simultaneous calculation of the Wagner diagram's variables and their graphical display.

The purpose of this paper is to present a newly-developed publicly and freely available application, the Helsinki O_2 Pathway Tool (HO_2PT), to import, calculate, graphically display, and export variables of the Wagner diagram. We believe this tool will advance the use of Wagner's and his colleagues' model and thereby the understanding of the physiological basis, limitations, and training- or disuse-induced adaptations of $\dot{V}O_{2max}$ and its components. For a more comprehensive and detailed physiological background of the current work, we encourage the reader to refer to the presented (e.g. Wagner 2008, 2011, 2020, 2023) and other related literature.

2. Methods

2.1. HO_2PT—aim, technical development, and functionalities

The HO_2PT is based on the integrated O_2 pathway model originally presented by Peter D. Wagner and his colleagues (Roca *et al* 1989, Wagner 1991, 1992, 2008, 2011, 2020, Esposito *et al* 2010). The model combines the Fick principle equation and Fick's law of diffusion to illustrate an integrated approach of convective and diffusive components of O_2 delivery, known as the Wagner diagram. The HO_2PT is intended to be used as a tool by anyone measuring $\dot{V}O_2$ and its components across the wide spectrum of contexts including scientific research, education, exercise testing, coaching, or clinical medicine.

Technical development of the HO_2PT was done as part of a Bachelor of Engineering thesis in cooperation between Helsinki Sports and Exercise Medicine Clinic (HULA), Sports and Exercise Medicine, Faculty of Medicine, University of Helsinki, and the School of Information and Communication Technology of Metropolia University of Applied Sciences in Helsinki, Finland (Mikkola 2022). The tool has been programmed in Python (www.python.org/) programming language and bundled to a cross-platform

software application with PyInstaller (https://pyinstaller.org/en/stable/), which makes running the HO_2PT possible in Windows, macOS, and Linux operating systems. The graphical user interface was developed using Python's Tkinter (https://docs.python.org/3/library/tkinter.html) interface for Tk graphical user interface toolkit. Other library dependencies the HO_2PT has are Numpy (https://numpy.org/) and Matplotlib (https://matplotlib.org/), that are used for the modeling, in addition to Pandas (https://pandas.pydata.org/) and Pandastable (https://pandastable.readthedocs.io/en/latest/description.html), that are used for data importing and exporting. Delivery of the HO_2PT, its source code, and user instructions (i.e. a detailed Operation Manual), are shared via GitHub (https://github.com/HO2PT/Helsinki-O2-Pathway-Tool/releases), which is a free online platform, and available also via the website of HULA (https://hula.fi/EP2/HO2PT).

The HO_2PT can be used to model O_2 pathway according to the Wagner diagram both quantitatively and graphically. Both user input data and data imported from a file with a data importer tool, specifically created for the application, can be used for modeling. In addition, the tool contains functionalities to modify and analyze the graphical results. For example, at an individual level, comparisons of individual's responses to exercise tests before and after any intervention can be made. At a group level, where utilizing the Wagner model and diagram has previously provided mechanistic insights into the determinants and adaptations of $\dot{V}O_{2max}$ in both health and disease (Esposito *et al* 2010, 2011, Wagner 2015, Houstis *et al* 2018, Broxterman *et al* 2020, 2021, 2024, Howden *et al* 2021, Legendre *et al* 2021, Manferdelli *et al* 2023), responses of one group can be modeled and illustrated, or responses of one group before and after any intervention or responses of two or several groups can be compared with each other. Basic statistical parameters (mean $\pm$ standard deviation or mean with 95% confidence intervals for normally distributed data; median with interquartile range for nonnormally distributed data) can be calculated for group-level data. Results of the modeling can be exported as image or spreadsheet files. Currently, there is no technical support for the source code. However, the source code of this tool is free to use and modifiable to fit one's individual needs and preferences.

2.2. HO_2PT—calculation

Variables and equations used in the HO_2PT are based on the original Wagner diagram and presented in table 1. Figure 2 illustrates a step-by-step flow chart for how the HO_2PT calculates its outputs. Regarding table 1, figure 2, and the equation of DO_2, while the original data of Roca *et al* (1989) show the constant k may slightly vary both intra- and interindividually along with prevailing circumstances, the same data also suggest it to be quite close to 2, and this is why the HO_2PT multiplies PvO_2 by 2 when the default setting is used. However, a user can instead input another individual value for k to be used for the calculation if one has experimentally determined such value. To complement further the information in table 1 and figure 2, the equations used for calculating PvO_2, corrected for venous blood temperature and pH, are based on Severinghaus's modified Hill equation (1979) and its direct solution for partial O_2 pressure (Ellis 1989) and are detailed in supplementary material 1.

2.3. HO_2PT—graphical display

For graphical display, the $\dot{V}O_2$ formulae need to be presented as a function of PvO_2. In terms of Fick's law of diffusion, PvO_2 is available in the formula. This is not the case, however, for the Fick principle, where $C(a\text{-}v)O_2$ must be split into its contributory factors. Consequently, the following formulae are used for the graphical display:

$$\dot{V}O_2 = DO_2 \times k \times PvO_2 \tag{4}$$

$$\dot{V}O_2 = \dot{Q} \times ((1.34 \times [Hb] \times SaO_2 + 0.03 \times PaO_2) - 1.34 \times [Hb] \times SvO_2) \tag{5}$$

where SaO_2 = arterial O_2 saturation, PaO_2 = partial arterial O_2 pressure, and SvO_2 = venous O_2 saturation. In terms of PaO_2, a user of the HO_2PT can choose from the tool's settings whether one includes PaO_2 in the equation (5) or not; in other words, the HO_2PT can also be used without data on PaO_2, and arterial O_2 content is in such case calculated as $1.34 \times [Hb] \times SaO_2$. In addition, the coefficient of PaO_2 in equation (5) is either 0.03 or 0.003 and depends on whether one uses ml O_2/l blood or ml O_2/dl blood, respectively, as a unit of arterial O_2 content.

Figure 1 illustrates a schematic graphical display of the relationship between $\dot{V}O_2$ and PvO_2. The curved Fick principle line in figure 1 plots $\dot{V}O_2$ as a function of PvO_2 and takes the shape of the oxyhemoglobin dissociation curve, albeit inverted; $\dot{V}O_2$ and PvO_2 must lie on this curved line as the Fick principle conveys the conservation of O_2 mass. In figure 1, the straight line, which illustrates Fick's law of diffusion and the slope of which represents DO_2, shows what $\dot{V}O_2$ (y-axis) should be in order that O_2 mass be conserved if

Table 1. Variables in the Helsinki O_2 Pathway Tool: abbreviations, units, procurement methods, and equations.

Variable	Abbreviation	Unit[a]	Method[b]	Equation[c]
Pulmonary O_2 uptake	$\dot{V}O_2$	• l/min • ml/min	• Measured • Calculated	• $\dot{Q} \times C\,(a\text{-}v)\,O_2$
Hemoglobin concentration	[Hb]	• g/l • g/dl	• Measured	
Arterial O_2 saturation	SaO_2	• %	• Measured	
Arterial O_2 content	CaO_2	• ml O_2/l blood • ml O_2/dl blood	• Measured • Calculated [d]	• $1.34 \times [Hb] \times SaO_2 + 0.03 \times PaO_2$ • $C(a\text{-}v)O_2 + CvO_2$
Partial arterial O_2 pressure	PaO_2	• mmHg	• Measured[e]	
Heart rate	HR	• bpm	• Measured	
Stroke volume	SV	• ml	• Measured • Calculated	• $\frac{\dot{V}O_2}{HR \times C(a\text{-}v)O_2}$
Cardiac output	$\dot{Q}$	• l/min	• Measured • Calculated	• $SV \times HR$ • $\frac{\dot{V}O_2}{C(a\text{-}v)O_2}$
Convective O_2 delivery	$\dot{Q}aO_2$	• ml/min	• Calculated	• $\dot{Q} \times CaO_2$
Arterial-venous O_2 difference	$C(a\text{-}v)O_2$	• ml O_2/l blood • ml O_2/dl blood	• Calculated	• $CaO_2 - CvO_2$ • $\frac{\dot{V}O_2}{\dot{Q}}$
Diffusive O_2 conductance	DO_2	• ml/min/mmHg	• Calculated[f]	• $\frac{\dot{V}O_2}{2 \times PvO_2}$
Venous O_2 saturation	SvO_2	• %	• Measured • Calculated	• $\frac{CaO_2 - C(a\text{-}v)O_2}{1.34 \times [Hb]}$
Venous O_2 content	CvO_2	• ml O_2/l blood • ml O_2/dl blood	• Measured • Calculated	• $1.34 \times [Hb] \times SvO_2$ • $CaO_2 - C(a\text{-}v)O_2$
Partial venous O_2 pressure	PvO_2	• mmHg	• Measured • Calculated	See supplementary material 1
(Venous) blood temperature	T	• °C • F • K	• Measured • Estimated	
(Venous) blood pH	pH		• Measured • Estimated	

[a] Variable-specific alternatives of units that can be used when using the Helsinki O_2 pathway tool (HO_2PT).
[b] Variable-specific alternatives of methods that can be used to procure needed data for using the HO_2PT.
[c] Variable-specific and method-dependent alternatives of equations that are used to quantify needed data when using the HO_2PT. See also figure 2 for the flow chart for how the HO_2PT step by step calculates its outputs.
[d] The HO_2PT can alternatively calculate CaO_2 without PaO_2 (i.e. $1.34 \times [Hb] \times SaO_2$). The coefficient of PaO_2, used by the HO_2PT, is either 0.03 or 0.003 and depends on whether one uses ml O_2/l blood or ml O_2/dl blood, respectively, as a unit of CaO_2.
[e] The HO_2PT can be used without any measured data on PaO_2 (see [d] above).
[f] The default equation to calculate DO_2 uses 2 for the constant k (i.e. the nominator in the default equation of DO_2 is: $2 \times PvO_2$), but a user can instead input another individual value for k to be used for the calculation if one has experimentally determined such value. See also text for details.

PvO_2 (x-axis) took any value between its lower limit (i.e. 0 mmHg) and upper limit of PaO_2. The straight line also defines the complete range of possible $\dot{V}O_2$ values across the range of possible PvO_2 values. In consequence, $\dot{V}O_2$ must lie somewhere on the straight line to maintain the conservation of O_2 mass, and

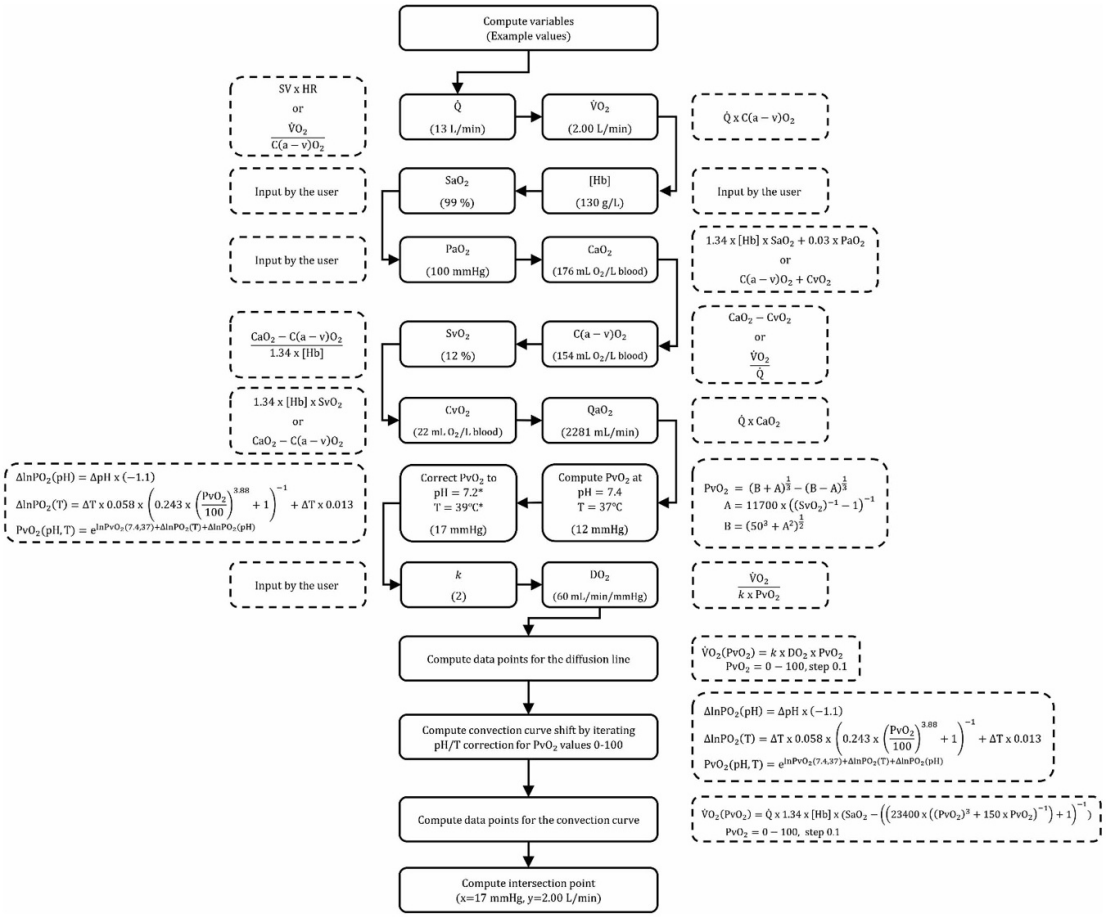

Figure 2. Flow chart illustrating how the Helsinki O_2 Pathway Tool (HO_2PT) performs its calculations from inputs to outputs. Example values of each variable of one individual's maximal exercise data are written in brackets. The boxes with dashed edges include either the note that a user inputs a value for a variable located in the adjacent box with solid edges or the equation(s) used for calculating each variable located in the adjacent box with solid edges. See text, table 1, and supplementary material 1 for details and the abbreviations. * 7.2 and 39 °C are examples of pH and temperature (T), for which partial venous O_2 pressure (PvO_2) can be corrected.

eventually, the two mass conservation equations (i.e. the Fick principle and Fick's law of diffusion) must result in the same $\dot{V}O_2$ at the same PvO_2, which is demonstrated by the intersection point of the curved and straight lines (Wagner 2008, 2011, 2020). Figure 2 illustrates how the HO_2PT proceeds from receiving inputs to the calculation of the particular intersection point and the graphical display.

2.4. HO_2PT—methods and data used during development

Data used during development of the tool have been collected at HULA and Sports and Exercise Medicine, Faculty of Medicine, University of Helsinki, Helsinki, Finland. To model and illustrate group-level data of healthy, normally-to-highly active men, we retrospectively used previously published data (Peltonen *et al* 2013). For individual-level analyses, we retrospectively used subjects ranging from clinical patients to elite athletes who have undergone comprehensive exercise testing described below. These subjects included but were not limited to individuals from our previously published studies (Peltonen *et al* 2013, Rissanen *et al* 2015, 2016, 2023), in which the individuals have represented both sexes, have been 19–46 year-old, have been either healthy or had disturbances in glucose-insulin homeostasis (i.e. type 1 diabetes, insulin resistance with no diabetes, polycystic ovary syndrome), and have had body mass index between 19 to 38 kg/m^2 and $\dot{V}O_{2max}$ between 16 to 61 ml/min/kg body mass. To demonstrate the effect of varying value of k on DO_2 during maximal cycling exercise at both group and individual levels, we used previously published data on premenopausal women with no diseases, medications, or other factors possibly affecting $\dot{V}O_{2max}$ (Rissanen *et al* 2023).

Two methods provided data for $\dot{V}O_2$ measurements: (i) ventilation measurements by a low-resistance volume turbine (Triple V, Jaeger Mijnhardt, Bunnik, The Netherlands) and inspired and expired gases by mass spectrometry (AMIS 2000, Innovision A/S, Odense, Denmark), and (ii) a low-resistance volume

turbine combined with an electrochemical fuel cell method to determine O_2 concentrations (Vyntus CPX, CareFusion, Hoechberg, Germany). Two versions of an impedance cardiography method were used to obtain stroke volume and $\dot{Q}$: (i) PhysioFlow PF-05 Lab1 (Manatec Biomedical, Paris, France), and (ii) PhysioFlow PF-07 Enduro (Manatec Biomedical, Paris, France). SaO_2 was monitored by pulse oximetry (Nonin 9600, Nonin Medical, Inc., Plymouth, MN) either from a fingertip or an earlobe. Measures for capillary blood [Hb] and pH were provided by blood gas analyzers (ABL725, Radiometer, Copenhagen, Denmark; ABL90 FLEX PLUS, Radiometer, Copenhagen, Denmark). Hb samples collected from the antecubital vein were analyzed in two local accredited laboratories (www.synlab.fi; https://huslab.fi).

In our laboratory, we have measured $\dot{V}O_2$ and $\dot{Q}$, and calculated $C(a\text{-}v)O_2$ according to the Fick principle. However, the HO_2PT can be used by providing measured values for any two of these variables to calculate the third one, and of course, all three variables can also be used as measured values (table 1). In addition, SaO_2 and [Hb] are needed for the calculations (table 1). In terms of venous blood temperature and pH, the values reflecting the existing venous conditions can be either directly measured or approximated according to the literature (e.g. Arngrimsson *et al* 2004, Mortensen *et al* 2005, González-Alonso *et al* 2015, Trangmar *et al* 2017). Regarding standard physiological conditions at rest, we have used $T = 37.0$ °C and pH = 7.4 in our example calculations.

3. Results

Based on the Python open source code and libraries, the HO_2PT was developed to model O_2 transport pathway both numerically and graphically according to the Wagner diagram. Figure 3 illustrates the data structure of the HO_2PT. The core of the HO_2PT is the App object acting as an interface between other objects. It contains information on the current status of the tool including an active project, subject, and exercise test. The App object also communicates with the Settings object that governs default settings. The most visible objects for the user are Project, Subject, and Test objects, that a user can create manually or import from an existing data file. Division of current data into three main categories is based on the nature of the research material: Each data set, which is modeled and analyzed, may contain various subjects with results from several exercise tests. Each test (Test) may have individual environmental conditions (EnvDetails) and subject's background information (SubjectDetails). In addition to data on maximal exercise, several workloads (Load) with individually measured and/or calculated values (WorkLoadDetails) can also be processed, although it deserves to be repeated here that it is only from near-maximal to maximal exercise when the graphical display is appropriate for the necessary assumptions to apply, as previously justified (see Introduction).

Figure 4 provides an overall user view of the HO_2PT. The left panel (panel 1) in figure 4 contains information on available project(s), subject(s), and exercise test(s). The panel's tools enable the user to create, edit, delete, and import data as well as add data to the graph. These functionalities enable the user to construct and analyze data freely from different sources. The top panel (panel 2) in figure 4 presents detailed information on active project(s) and test(s) and allows user to modify settings for graphical display. The modeling is based on the information provided in the top panel and its graphical and numerical results are provided in a tab in the bottom panel (panel 3). The bottom panel is divided into the graphical results and its tools and the numerical values. The panel presents data according to the Wagner diagram and the corresponding numerical values are visible on a separate tab next to the graph. The user can separately edit the appearance of the diagrams by controlling their visibility, line type, and line color. The user can also modify the graph title, numbers of ticks, and scales of axes, and when finished, save the graphical result as an image file (.png). The numerical results provide an option for the user to edit the units and information about the method (i.e. measured or calculated) used for data collection. Both the graphical and numerical results can be exported into a spreadsheet file.

Figures 5 and 6 demonstrate examples of group- and individual-level data. Figure 5 provides an example of group-level data (medians) on healthy, normally-to-highly active men during maximal cycling exercise. Figure 6 provides an example of maximal exercise responses of a male cross-country skier before and after a 4-week 'Living High-Training High and Low' camp.

Supplementary material 2 demonstrates the effect of varying value of k on DO_2 during maximal exercise at both group and individual levels. At group level, DO_2 during maximal exercise does not differ between a situation where k constantly equals 2 and a situation where k randomly varies from 1.8 to 2.2. At individual level, compared to a situation where k equals 2, DO_2 during maximal exercise is 11% higher, 5% higher, 5% lower, or 9% lower if k equals 1.8, 1.9, 2.1, or 2.2, respectively.

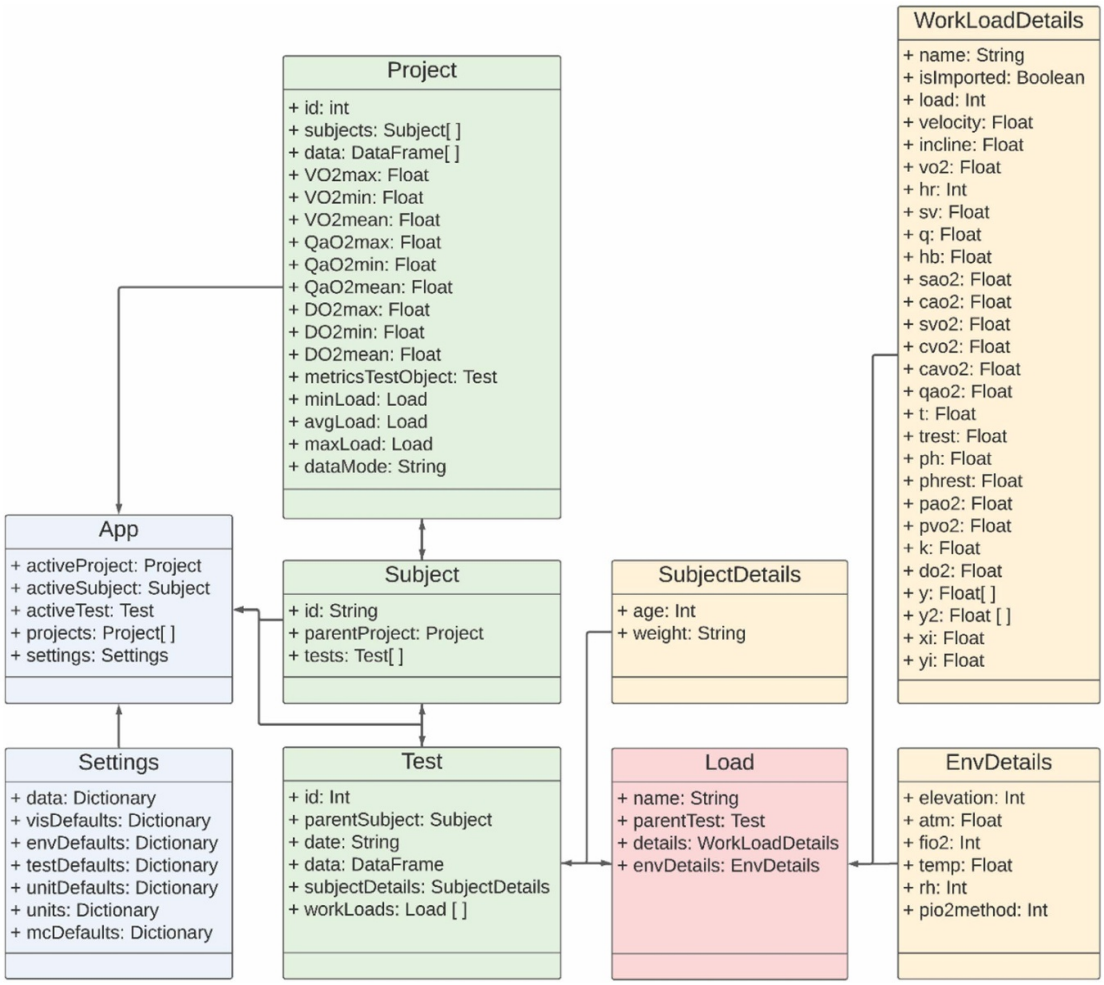

Figure 3. Data structure of the Helsinki O_2 Pathway Tool (HO_2PT). Light blue objects (App, Settings) act as interfaces enabling data access and storage between objects. Light green objects (Project, Subject, Test) are the main three objects that are based on the nature of the research data. The red object (Load) acts as a workload or a step of a test. Yellow objects (SubjectDetails, WorkLoadDetails, EnvDetails) contain more detailed information about its respective parent object.

4. Discussion

4.1. Perspective and novelty

Since Peter D. Wagner and his colleagues presented the Wagner diagram (Roca *et al* 1989, Wagner 1991, 1992), and then later examined and clarified it further (Wagner 2008, 2011, 2020, 2023), it has been clear that instead of asking which single step of O_2 pathway limits $\dot{V}O_{2max}$, the processes of O_2 transport and utilization should be approached from the perspective of an integrated system. This has been perhaps most strikingly demonstrated in patients, who suffer from some specific cardiorespiratory condition such as heart failure (Esposito *et al* 2010, 2011, Houstis *et al* 2018, Nayor *et al* 2020, Legendre *et al* 2021), chronic obstructive pulmonary disease (Broxterman *et al* 2020, 2021), or chronic thromboembolic pulmonary hypertension (Howden *et al* 2021), but whose exercise tolerance and $\dot{V}O_{2max}$ are multifactorially limited by several derangements throughout the integrated O_2 pathway. In addition to diseases, also aging exposes to multifactorial limitations to $\dot{V}O_{2max}$ (Valenzuela *et al* 2020). Furthermore, both exercise training and skeletal muscle disuse influence multiple components of $\dot{V}O_{2max}$ instead of an influence on some single component (Esposito *et al* 2011, Wagner 2015, Broxterman *et al* 2021, 2024, Legendre *et al* 2021). However, to our knowledge, there have been no publicly available tools providing access to simultaneous calculation of the Wagner diagram's multiple variables and their graphical display. This paper presents the HO_2PT, to import, calculate, graphically display, and export variables of the Wagner diagram, which brings the components of the O_2 transport pathway into one model and graph.

In the HO_2PT, both user input data and data imported from a file with the created data importer tool can be used for modeling. In addition, the tool contains functionalities to modify and analyze the numerical and graphical results. The HO_2PT is an open source application. The source code of the tool has been created

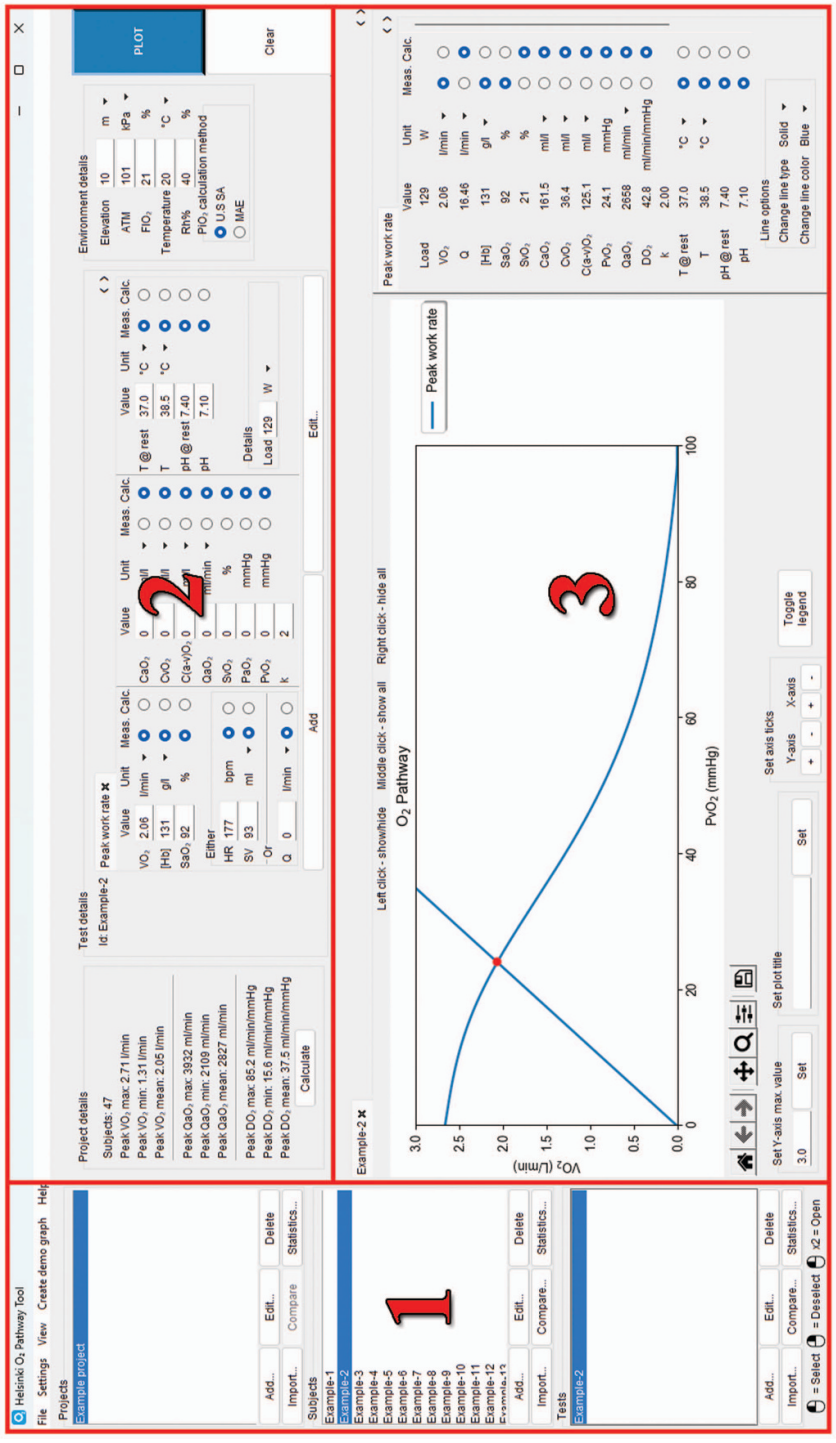

Figure 4. User view of the Helsinki O_2 Pathway Tool (HO_2PT) to calculate variables of the Wagner diagram. See text for the details of the overall view. The graph and related data in the panels 2 and 3 represent maximal cycling exercise responses of a 29-year-old woman with no chronic diseases.

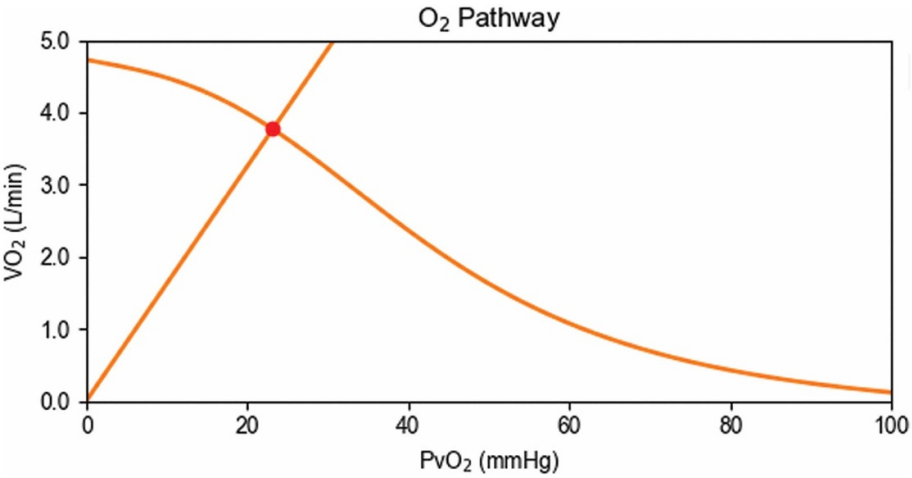

Figure 5. Maximal cycling in healthy, nonsmoking, and normally-to-highly active men ($N = 10$, age 30.7 ± 5.5 years [mean ± SD], height 185.0 ± 7.0 cm, body mass 84.0 ± 10.1 kg, body mass index 24.5 ± 2.1 kg/m^2, body fat 14.1 ± 4.2%). Group-level data are presented as medians. Medians for $\dot{V}O_{2max}$, $\dot{Q}_{max}$, SaO_2 during maximal exercise, and [Hb] are 3.85 l/min, 24.6 l/min, 95%, and 151 g/l, respectively, and based on previously published data (Peltonen *et al* 2013). With these values, HO_2PT returns a median maximal PvO_2 of 24 mmHg and a median maximal DO_2 of 73 ml/min/mmHg. Mean venous blood pH and temperature during maximal exercise were here approximated to be 7.10 (corresponding to an average of values 7.03 and 7.17 reported in Mortensen *et al* (2005) and Trangmar *et al* (2017)) and 38.5 °C (González-Alonso *et al* 2015), respectively.

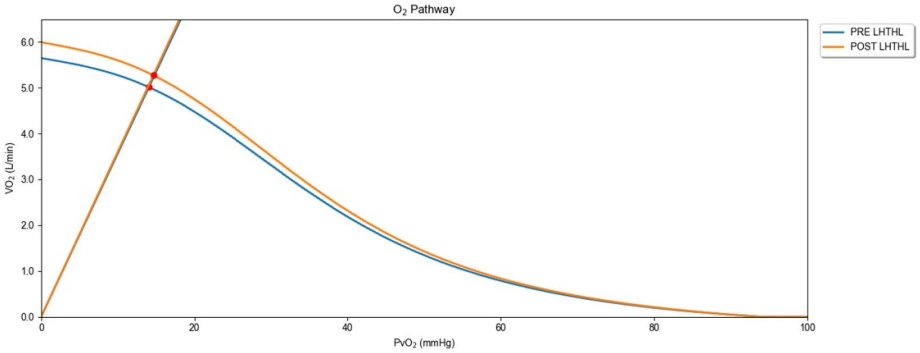

Figure 6. Results of a male cross-country skier during Nordic walking/running on a treadmill before (blue lines) and after (orange lines) a 4-week 'Living High-Training High and Low' (LHTHL) camp. $\dot{V}O_{2max}$ (5.01 and 5.27 l/min), $\dot{Q}_{max}$ (31.8 and 30.9 l/min), SaO_2 (94 and 94%), [Hb] (141 and 154 g/l), and blood pH during maximal exercise (7.24 and 7.24) were measured before and after LHTHL, respectively. With these values, HO_2PT returns DO_2 values of 178 and 180 ml/min/mmHg and PvO_2 values of 14 and 15 mmHg before and after LHTHL, respectively. Noteworthily, pH was measured here from capillary blood (instead of venous blood) and these measured pH data must thus be regarded as rough approximate values. Venous blood temperature during maximal exercise was here approximated to be 38.5 °C (González-Alonso *et al* 2015) in both tests.

with Python and its additional libraries, the tool is distributed via GitHub online platform and HULA website (see Methods for the internet addresses), and can be run as a desktop application within Windows, macOS, and Linux operating systems. This makes the tool freely and widely available as well as modifiable to fit one's individual needs.

4.2. Methodological considerations

Any tool like the HO_2PT must be based on specific assumptions as Wagner's and his colleagues' model covers the complex interplay between the atmosphere and numerous organ systems. Consequently, also the HO_2PT has its limitations.

First, in its current form, the tool pertains only to such conditions under which the mitochondrial oxidative capacity is higher than the capacity of the O_2 transport system to deliver O_2 to the mitochondria. While this is likely the case among trained individuals (Knight *et al* 1993, Gifford *et al* 2016) and although Boushel *et al* (2011) have reported that this might also hold true for sedentary individuals, there is a theoretical framework (Cano *et al* 2013) combined to scientific evidence (Cardús *et al* 1998, Jacobs *et al* 2013, Gifford *et al* 2016, Broxterman *et al* 2024) to support the contention that mitochondrial oxidative capacity may be a significant source of limitation to $\dot{V}O_{2max}$ of an untrained individual. From a methodological

perspective, there is currently a lack of such practically feasible methodology that would enable the inclusion of the mitochondrial measures in the HO_2PT calculations. However, mitochondrial limitation to $\dot{V}O_{2max}$ can of course be revealed if an individual performs repeated exercise tests in normoxia and hyperoxia and achieves equal levels of $\dot{V}O_{2max}$ (or exercise capacity) under the two circumstances (Cardús *et al* 1998, Broxterman *et al* 2024).

Second, the tool calculates DO_2 to quantify the diffusive O_2 conductance (or capacity) in skeletal muscle but does so based on $\dot{V}O_2$ and $\dot{Q}$ determined at the whole-body level. This is a limitation as although it is physiologically justified to use the Wagner diagram only from near-maximal to maximal exercise, during which the substantial portion of $\dot{Q}$ is redistributed to active skeletal muscles where the vast majority of O_2 consumption takes place (Laughlin *et al* 2012), calculating 'muscle-level' DO_2 based on $\dot{V}O_2$ and $\dot{Q}$ determined at whole-body level tends to lead to an overestimation of the actual muscle diffusion. This limitation must be acknowledged when one draws (patho)physiological conclusions based on DO_2 data calculated as the tool does. It deserves to be mentioned here that also muscle-specific DO_2 can be quantified but it would require either noninvasive near-infrared spectroscopy (Pilotto *et al* 2022), invasive measurement of blood flow as well as local arterial and venous O_2 (Andersen and Saltin 1985, Roca *et al* 1989), or positron emission tomography imaging (Kalliokoski *et al* 2001). In addition, direct DO_2 quantification is more feasible for isolated muscle exercise than whole-body exercise and impractical from the perspective of daily exercise testing and clinical practice.

Third, the default equation to calculate DO_2 is based on the assumption that the constant k equals 2. This is not exactly correct as while k is likely close to 2, it may vary both intra- and interindividually along with prevailing circumstances (Roca *et al* 1989, Esposito *et al* 2010, Broxterman *et al* 2021). The aim of this assumption is to increase the usability of the HO_2PT as determining an exact and individual k value for each individual would require several experiments under varying circumstances per each individual and invasive blood samples drawn during such experiments, which might substantially elevate the threshold to use the tool. Importantly, however, a user of the HO_2PT can instead input another individual value for k to be used for the calculation if one has experimentally determined such value. The sensitivity analysis presented in supplementary material 2 demonstrates how DO_2 during maximal exercise does not differ at group level between a situation where k constantly equals 2 and a situation where k randomly varies around 2. On the other hand, the sensitivity analysis at individual level demonstrates how an individual's DO_2 during maximal exercise is affected approximately $\pm$10% if k is 10% lower or higher than 2.

Fourth, it is noteworthy that we have developed the HO_2PT with data that we have collected with our specific noninvasive methods and devices (see Methods). Thus, we regard it as important that the usability of the HO_2PT would be tested further also in laboratories utilizing various methods and in various contexts extending from clinical populations to elite athletes. Importantly, such future research should include testing the validity of the tool against the Bohr forward integration method, which requires invasively collected arterial and venous blood samples to estimate mean $PcapO_2$ and then calculate muscle-level DO_2 as a quotient of $\dot{V}O_2$ and mean $PcapO_2$ (Roca *et al* 1989).

5. Conclusion

Here we have presented the newly-developed publicly and freely available HO_2PT application to import, calculate, graphically display, and export variables of the Wagner diagram, which brings the components of the O_2 transport pathway into one model and graph. While the HO_2PT is based on the previously published theory and equations, its novelty resides in providing a functional and demonstrative platform for those interested in examining $\dot{V}O_{2max}$ and its determinants by using the Wagner diagram. As any technical application aiming to model complex and integrated physiological phenomena, also the HO_2PT has its limitations. However, we overall believe the HO_2PT will lower the threshold to approach and take advantage of Wagner's and his colleagues' integrated model and thereby benefit users across the wide spectrum of experts in the fields of scientific research, education, exercise testing, sports coaching, and clinical medicine.

Data availability statement

No new data were collected for this study.

The data cannot be made publicly available upon publication because they are not available in a format that is sufficiently accessible or reusable by other researchers. The data that support the findings of this study are available upon reasonable request from the authors.

Acknowledgments

We would like to thank Professor Etienne Gagnon from Franklin & Marshall College, Lancaster, PA, USA, for his guidance on graphical display modeling presented in the manuscript.

Funding for this study was provided by Ministry of Education and Culture, Finland (OKM/128/626/2021; OKM/39/626/2022), and Urheiluopistosäätiö.

The authors declare no conflicts of interest.

Ethical statement

All subjects, the data on whom have been retrospectively used for developing the HO_2PT, have provided their oral and written informed consents to allow the use of their data for scientific purposes, and all specific research projects at HULA and Sports and Exercise Medicine, Faculty of Medicine, University of Helsinki have been conducted according to the guidelines of the Declaration of Helsinki and approved by the appropriate ethics committees.

ORCID iD

Antti-Pekka E Rissanen https://orcid.org/0000-0003-2415-3979

References

Andersen P and Saltin B 1985 Maximal perfusion of skeletal muscle in man *J. Physiol.* **366** 233–49

Arngrimsson S A, Petitt D, Borrani F, Skinner K and Cureton K 2004 Hyperthermia and maximal oxygen uptake in men and women *Eur. J. Appl. Physiol.* **92** 524–32

Boushel R, Gnaiger E, Calbet J A L, Gonzalez-Alonso J, Wright-Paradis C, Sondergaard H, Ara I, Helge J W and Saltin B 2011 Muscle mitochondrial capacity exceeds maximal oxygen delivery in humans *Mitochondrion* **11** 303–7

Broxterman R M, Hoff J, Wagner P D and Richardson R S 2020 Determinants of the diminished exercise capacity in patients with chronic obstructive pulmonary disease: looking beyond the lungs *J. Physiol.* **598** 599–610

Broxterman R M, Wagner P D and Richardson R S 2021 Exercise training in COPD: muscle O_2 transport plasticity *Eur. Respir. J.* **58** 2004146

Broxterman R M, Wagner P D and Richardson R S 2024 Endurance exercise training changes the limitation on muscle $\dot{V}O_{2max}$ in normoxia from the capacity to utilize O_2 to the capacity to transport O_2 *J. Physiol.* **602** 445–59

Cano I, Mickael M, Gomez-Cabrero D, Tegnér J, Roca J and Wagner P D 2013 Importance of mitochondrial PO_2 in maximal O_2 transport and utilization: a theoretical analysis *Respir. Physiol. Neurobiol.* **189** 189 477–83

Cardús J, Marrades R M, Roca J, Barbera J A, Diaz O, Masclans J R, Rodriguez-roisin R and Wagner P D 1998 Effects of F_IO_2 on leg $\dot{V}O_2$ during cycle ergometry in sedentary subjects *Med. Sci. Sports Exerc.* **30** 697–703

Ellis R K 1989 Determination of PO_2 from saturation *J. Appl. Physiol.* **67** 902

Esposito F, Mathieu-Costello O, Shabetai R, Wagner P D and Richardson R S 2010 Limited maximal exercise capacity in patients with chronic heart failure: partitioning the contributors *J. Am. Coll. Cardiol.* **55** 1945–54

Esposito F, Reese V, Shabetai R, Wagner P D and Richardson R S 2011 Isolated quadriceps training increases maximal exercise capacity in chronic heart failure: the role of skeletal muscle convective and diffusive oxygen transport *J. Am. Coll. Cardiol.* **58** 1353–62

Fick A 1870 Über die Messung des Blutquantums in den Herzventrikeln *Sitzber. Phys. Med. Ges. Würzburg* 290–1

Gayeski T E and Honig C R 1986 O_2 gradients from sarcolemma to cell interior in red muscle at maximal $\dot{V}O_2$ *Am. J. Physiol.* **251** H789–99

Gifford J R *et al* 2016 Symmorphosis and skeletal muscle $\dot{V}O_{2max}$: in vivo and in vitro measures reveal differing constraints in the exercise-trained and untrained human *J. Physiol.* **594** 1741–51

Gifford J R, Blackmon C, Hales K, Hinkle L J and Richards S 2024 Overdot and overline annotation must be understood to accurately interpret $\dot{V}O_{2max}$ physiology with the Fick formula *Front. Physiol.* **15** 1359119

González-Alonso J, Calbet J A L, Boushel R, Helge J W, Søndergaard H, Munch-Andersen T, van Hall G, Mortensen S P and Secher N H 2015 Blood temperature and perfusion to exercising and non-exercising human limbs *Exp. Physiol.* **100** 1118–31

Hirai D M, Musch T I and Poole D C 2015 Exercise training in chronic heart failure: improving skeletal muscle O_2 transport and utilization *Am. J. Physiol. Heart. Circ. Physiol.* **309** H1419–39

Houstis N E, Eisman A S, Pappagianopoulos P P, Wooster L, Bailey C S, Wagner P D and Lewis G D 2018 Exercise intolerance in heart failure with preserved ejection fraction: diagnosing and ranking its causes using personalized O_2 pathway analysis *Circulation* **137** 148–61

Howden E J *et al* 2021 Oxygen pathway limitations in patients with chronic thromboembolic pulmonary hypertension *Circulation* **143** 2061–73

Jacobs R A, Flück D, Bonne T C, Bürgi S, Christensen P M, Toigo M and Lundby C 2013 Improvements in exercise performance with high-intensity interval training coincide with an increase in skeletal muscle mitochondrial content and function *J. Appl. Physiol.* **115** 785–93

Kalliokoski K K, Oikonen V, Takala T O, Sipilä H, Knuuti J and Nuutila P 2001 Enhanced oxygen extraction and reduced flow heterogeneity in exercising muscle in endurance-trained men *Am. J. Physiol. Endocrinol. Metab.* **280** E1015–21

Knight D R, Schaffartzik W, Poole D C, Hogan M C, Bebout D E and Wagner P D 1993 Effects of hyperoxia on maximal leg O_2 supply and utilization in men *J. Appl. Physiol.* **75** 2586–94

Koch L G and Britton S L 2008 Aerobic metabolism underlies complexity and capacity *J. Physiol.* **586** 83–95

Laughlin M H *et al* 2012 Peripheral circulation *Compr. Physiol.* **2** 321–447

Legendre A, Moatemri F, Kovalska O, Balice-Pasquinelli M, Blanchard J-C, Lamar-Tanguy A, Ledru F, Cristofini P and Iliou M-C 2021 Responses to exercise training in patients with heart failure. Analysis by oxygen transport steps *Int. J. Cardiol.* **330** 120–7

Levine B D 2008 $\dot{V}O_{2max}$: what do we know, and what do we still need to know? *J. Physiol.* **586** 25–34
Manferdelli G, Narang B J, Bourdillon N, Debevec T and Millet G P 2023 Physiological responses to exercise in hypoxia in preterm adults: convective and diffusive limitations in the O_2 transport *Med. Sci. Sports Exerc.* **55** 482–96
Mikkola T 2022 *Helsinki O_2 Pathway Tool: Quantitative and Graphical Modeling of Oxygen Pathway* (Metropolia University of Applied Sciences)
Millet G P, Burtscher J, Bourdillon N, Manferdelli G, Burtscher M and Sandbakk Ø 2023 The $\dot{V}O_{2max}$ legacy of Hill and Lupton (1923)-100 years on *Int. J. Sports Physiol. Perform.* **18** 1362–5
Mortensen S P, Dawson E A, Yoshiga C C, Dalsgaard M K, Damsgaard R, Secher N H and González-Alonso J 2005 Limitations to systemic and locomotor limb muscle oxygen delivery and uptake during maximal exercise in humans *J. Physiol.* **566** 273–85
Nayor M, Houstis N E, Namasivayam M, Rouvina J, Hardin C, Shah R V, Ho J E, Malhotra R and Lewis G D 2020 Impaired exercise tolerance in heart failure with preserved ejection fraction: quantification of multiorgan system reserve capacity *JACC Heart Fail.* **8** 605–17
Peltonen J E, Hägglund H, Koskela-Koivisto T, Koponen A S, Aho J M, Rissanen A-P E, Shoemaker J K, Tiitinen A and Tikkanen H O 2013 Alveolar gas exchange, oxygen delivery and tissue deoxygenation in men and women during incremental exercise *Respir. Physiol. Neurobiol.* **188** 102–12
Pilotto A M *et al* 2022 Near-infrared spectroscopy estimation of combined skeletal muscle oxidative capacity and O_2 diffusion capacity in humans *J. Physiol.* **600** 4153–68
Poole D C, Behnke B J and Musch T I 2021 The role of vascular function on exercise capacity in health and disease *J. Physiol.* **599** 889–910
Poole D C and Musch T I 2008 Solving the Fick principle using whole body measurements does not discriminate 'central' and 'peripheral' adaptations to training *Eur. J. Appl. Physiol.* **103** 117–9
Poole D C, Musch T I and Colburn T D 2022 Oxygen flux from capillary to mitochondria: integration of contemporary discoveries *Eur. J. Appl. Physiol.* **122** 7–28
Poole D C and Richardson R S 1997 Determinants of oxygen uptake. Implications for exercise testing *Sports Med.* **24** 308–20
Richardson R S, Noyszewski E A, Kendrick K F, Leigh J S and Wagner P D 1995 Myoglobin O_2 desaturation during exercise. Evidence of limited O_2 transport *J. Clin. Invest.* **96** 1916–26
Rissanen A P, Tikkanen H O, Koponen A, Aho J M and Peltonen J E 2015 Central and peripheral cardiovascular impairments limit $\dot{V}O_{2peak}$ in type 1 diabetes *Med. Sci. Sports Exerc.* **47** 223–30
Rissanen A-P E, Koskela-Koivisto T, Hägglund H, Koponen A, Aho J M, Pöyhönen-Alho M, Tiitinen A, Tikkanen H O and Peltonen J E 2016 Altered cardiorespiratory response to exercise in overweight and obese women with polycystic ovary syndrome *Physiol. Rep.* **4** e12719
Rissanen A, Rissanen J, Pöyhönen-Alho M, Tiitinen A, Tikkanen H O, Shoemaker J K, Petrella R and Peltonen J E 2023 Insulin resistance without coexisting hyperglycaemia is not independently associated with cardiorespiratory fitness or its components: a retrospective cross-sectional study *Eur. Heart J.* **44** ehad655.2587
Roca J, Hogan M C, Story D, Bebout D E, Haab P, Gonzalez R, Ueno O and Wagner P D 1989 Evidence for tissue diffusion limitation of $\dot{V}O_{2max}$ in normal humans *J. Appl. Physiol.* **67** 291–9
Ross R *et al* 2016 Importance of assessing cardiorespiratory fitness in clinical practice: a case for fitness as a clinical vital sign: a scientific statement from the American Heart Association *Circulation* **134** e653–99
Rowell L B 1986 *Human Circulation Regulation During Physical Stress* (Oxford University Press)
Severinghaus J W 1979 Simple, accurate equations for human blood O_2 dissociation computations *J. Appl. Physiol.* **46** 599–602
Trangmar S J, Chiesa S T, Kalsi K K, Secher N H and González-Alonso J 2017 Whole body hyperthermia, but not skin hyperthermia, accelerates brain and locomotor limb circulatory strain and impairs exercise capacity in humans *Physiol. Rep.* **5** e13108
Valenzuela P L, Maffiuletti N A, Joyner M J, Lucia A and Lepers R 2020 Lifelong endurance exercise as a countermeasure against age-related $\dot{V}O_{2max}$ decline: physiological overview and insights from masters athletes *Sports Med.* **50** 703–16
Wagner P D 1991 Central and peripheral aspects of oxygen transport and adaptations with exercise *Sports Med.* **11** 133–42
Wagner P D 1992 Gas exchange and peripheral diffusion limitation *Med. Sci. Sports Exerc.* **24** 54–58
Wagner P D 2008 Systemic oxygen transport and utilization *J. Breath Res.* **2** 024001
Wagner P D 2011 Modeling O_2 transport as an integrated system limiting $\dot{V}O_{2max}$ *Comput. Methods Prog. Biomed.* **101** 109–14
Wagner P D 2015 A re-analysis of the 1968 Saltin *et al* "Bedrest" paper *Scand. J. Med. Sci. Sports* **25** 83–87
Wagner P D 2023 Determinants of maximal oxygen consumption *J. Muscle Res. Cell Motil.* **44** 73–88
Wagner P D 2020 Oxygen transport from air to tissues as an integrated system: what limits maximal O_2 *Consumption in Health and Disease? Structure-Function Relationships in Various Respiratory Systems, Respiratory Disease Series: Diagnostic Tools and Disease Managements* ed K Yamaguchi (Springer) pp 191–217